

Electronic transport in graphene: A semiclassical approach including midgap states

T. Stauber,¹ N. M. R. Peres,² and F. Guinea¹

¹*Instituto de Ciencia de Materiales de Madrid, CSIC, Cantoblanco, E-28049 Madrid, Spain*

²*Center of Physics and Department of Physics, University of Minho, P-4710-057 Braga, Portugal*

(Received 19 July 2007; revised manuscript received 19 September 2007; published 20 November 2007)

Using the semiclassical Boltzmann theory, we calculate the conductivity as a function of the carrier density. We include the scattering from charged impurities but conclude that the estimated impurity density is too low in order to explain the experimentally observed mobilities. We thus propose an additional scattering mechanism involving midgap states, which leads to a similar k dependence of the relaxation time as charged impurities. The proposed scattering mechanism can account for the experimental findings such as the sublinear behavior of the conductivity versus gate voltage and the increase of the minimal conductivity for clean samples. We also discuss temperature dependent scattering due to acoustic phonons.

DOI: [10.1103/PhysRevB.76.205423](https://doi.org/10.1103/PhysRevB.76.205423)

PACS number(s): 72.10.-d, 72.15.Jf, 72.15.Lh, 65.40.-b

I. INTRODUCTION

Electronic transport through two-dimensional graphene sheets has attracted incessant attention ever since the first experimental measurements on a Hall geometry were performed by Novoselov *et al.* about three years ago.¹ This is due to some spectacular findings such as the universal minimal conductivity at the Dirac point and the high mobility of the samples, which is basically independent of doping and temperature.^{2,3} Different experimental setups, i.e., electrical field¹ versus chemical doping,⁴ also give rise to different theoretical models. For recent qualitative reviews on both the experimental and theoretical status of the field, see Refs. 5–8.

So far, the scattering mechanism which determines the transport properties has not unambiguously been identified, but there is a strong evidence that long-range Coulomb scatterers can account for many of the experimental findings.^{9–12} It was shown within the Boltzmann formalism that the conductivity scales linearly with the carrier density if one assumes charged impurities in the SiO₂ substrate close to the graphene sheet.⁹ This semiclassical approach was also applied to systems close to the Dirac point and in the presence of adsorbed molecules.¹³

Recently, it was claimed that a Boltzmann theory with long-range Coulomb scatterers can account for all experimental findings if one renormalizes the carrier density close to the Dirac point due to potential fluctuations.^{14,15} The theory predicts a nonuniversal behavior of the minimal conductivity at the Dirac point, which nevertheless coincides with the experimentally observed value of $4e^2/h$ for “dirty” samples. This is in contrast to numerical studies based on the Kubo formalism by Nomura and MacDonald,¹⁶ who show that the conductivity is a function of n/n_i with n_i the impurity density, thus finding a universal behavior when the carrier density n goes to zero. The main criticism of Ref. 14 is the high density of charged impurities $n_i \gtrsim 10^{12}$ cm⁻² needed to match the experimentally observed mobilities, not likely to be present in an insulator such as SiO₂.¹⁷

In this paper, we propose an additional scattering mechanism originating from midgap states, which may be formed due to vacancies, cracks, boundaries, or impurities in the

substrate with a high potential difference with respect to the graphene sheet.^{18,19} They also occur in corrugated graphene.²⁰ The phase shift resulting from these types of disorder must approach zero for wave vectors close to the Dirac point. In contrast to the phase shift due to a short-range contact potential, this behavior is not linear but logarithmic.^{21,22} The resulting scattering time is, therefore, proportional to k up to logarithmic corrections. It is interesting to note that this behavior is also found for a two-dimensional (“nonrelativistic”) electron gas²² and in corrugated graphene²³ where the focus was laid on the resulting random gauge field.

Within the Boltzmann approach, the new mechanism can account for (a) quasiuniversal minimal conductivity for dirty samples, (b) a higher minimal conductivity for cleaner samples, and (c) sublinear behavior of the conductivity as a function of the gate voltage. We further obtain realistic values for the mobility assuming an equal concentration for Coulomb scatterers and vacancies of order $n_i \sim 10^{10} - 10^{11}$ cm⁻².

The paper is organized as follows. In Sec. II, we will first introduce the Boltzmann approach and comment on its applicability to graphene, i.e., to chiral Dirac fermions. In Sec. III, we discuss the density of states in the presence of midgap states needed to estimate the transport properties close to the Dirac point. In Sec. IV, we calculate the relaxation time and electrical conductivity for the various scattering mechanism including acoustical phonons. In Sec. V, we discuss the ac conductivity, the thermal conductivity and the thermopower for the scattering mechanism including midgap states and present numerical results in Sec. VI. We close with conclusions and remarks.

II. BOLTZMANN EQUATION

A. Collision-free Boltzmann equation

We start by showing that the Boltzmann equation description leads to the same plasmon spectrum as the more used many-body methods.^{24,25} This shows that a semiclassical approach for the transport properties of graphene is accurate.

The Boltzmann equation is described in terms of the electronic distribution function $f_{\mathbf{k}}$. Within this semiclassical ap-

proach, f_k depends on space \mathbf{r} and time t , i.e.,

$$f_k = f_{k(t)}(\mathbf{r}, t). \quad (1)$$

Looking at time scales shorter than the lifetime of the quasiparticles, the number of quasiparticles in the state \mathbf{k} is conserved. Via the continuity equation $\dot{f}_k + \nabla_r \cdot \mathbf{j}_k = 0$ with $\mathbf{j}_k = \mathbf{v}_k f_k$ denoting the particle current, one arrives at the collision-free Boltzmann equation. With $\dot{\mathbf{k}} = e \nabla_r \varphi$, where φ is the scalar potential of the internal electrical field, this reads in Fourier space as²⁶

$$(-i\omega + i\mathbf{q} \cdot \mathbf{v}_k) f_k(\mathbf{q}, \omega) = ie\mathbf{q} \cdot \mathbf{v}_k \left(-\frac{\partial f_k}{\partial \epsilon_k} \right) \varphi(\mathbf{q}, \omega). \quad (2)$$

To investigate screening properties, an external potential $\varphi^{ext}(\mathbf{q}, \omega)$ is assumed. To linear order in the total potential φ , the induced density is then given by

$$\rho^{ind}(\mathbf{q}, \omega) = \frac{4}{A} \sum_k \frac{\mathbf{q} \cdot \mathbf{v}_k}{\omega - \mathbf{q} \cdot \mathbf{v}_k} \left(-\frac{\partial f_k^0}{\partial \epsilon_k} \right) [-e\varphi(\mathbf{q}, \omega)], \quad (3)$$

where A is the area of the graphene sheet and spin and valley degeneracies have been included.

The induced potential is obtained by $(-e)\varphi^{ind}(\mathbf{q}, \omega) = V_q \rho^{ind}(\mathbf{q}, \omega)$ with $V_q = \frac{1}{2\epsilon_0 q}$ the two-dimensional Fourier transform of the Coulomb potential. For the dielectric function $\epsilon(\mathbf{q}, \omega) = \varphi^{ext}(\mathbf{q}, \omega) / \varphi(\mathbf{q}, \omega)$, one then obtains in the long-wavelength limit $v_F q \ll \omega$ the following expression:

$$\epsilon(\mathbf{q}, \omega) \approx 1 - \frac{V_q}{\omega^2} \frac{4}{A} \sum_k (\mathbf{q} \cdot \mathbf{v}_k)^2 \left(-\frac{\partial f_k^0}{\partial \epsilon_k} \right) = 1 - \frac{V_q}{\omega^2} \frac{q^2 \epsilon_F}{\pi}. \quad (4)$$

Plasmon excitations are given by $\epsilon(\mathbf{q}, \omega) = 0$, which leads to the plasmon dispersion

$$\omega = \sqrt{\frac{e^2}{2\pi\epsilon_0} \epsilon_F q}. \quad (5)$$

This relation including the prefactor is also obtained from a standard tight-binding model of graphene, where the dielectric function is calculated within the random-phase approximation.^{24,25} Our subsequent results should thus be valid even close to the neutrality point as long as $k_F \ell \gg 1$ (ℓ the mean free path), i.e., the chirality of the Dirac fermions only enters in the expression for the transition rate [see Eq. (21)]. For a quantitative analysis starting from a two-band model, see Ref. 27.

B. Collision term

We now include the possibility of changing the quantum state \mathbf{k} by introducing a collision term which is usually facilitated by the relaxation-time approximation,²⁸

$$-\frac{\partial f_k}{\partial t} \Big|_{\text{scatt}} \rightarrow \frac{g_k}{\tau_k}, \quad (6)$$

where $f_k - f_k^0 = g_k$.

Applying an electric field \mathbf{E} to the sample, the solution of the linearized Boltzmann equation then reads

$$g_k = -\frac{\partial f^0(\epsilon_k)}{\partial \epsilon_k} e\tau_k \mathbf{v}_k \cdot \mathbf{E}, \quad (7)$$

and the electric current reads

$$\mathbf{J} = \frac{4}{A} \sum_k e\mathbf{v}_k g_k. \quad (8)$$

Since at low temperature the following relation $-f^0(\epsilon_k) / \partial \epsilon_k \rightarrow \delta[v_F \hbar(k - k_F)]$ holds, we obtain for the conductivity with the Fermi velocity v_F the well-known formula⁹

$$\sigma = \frac{e^2 v_F^2}{2} \rho(E_F) \tau_{k_F}. \quad (9)$$

In the following, we will give expressions for the density of states $\rho(E)$ and the relaxation time τ_k . We then discuss the electrical conductivity in the low- and high-density limits.

III. DENSITY OF STATES

The density of states per unit area of clean graphene is given by

$$\rho_0(E) = \frac{2|E|}{\pi(\hbar v_F)^2}, \quad (10)$$

where spin and valley degeneracies have been included.

Due to potential disorder, this linear behavior becomes sublinear,²⁹ though the density of states at the Dirac point is still zero. More important are local defects in the form of vacancies, which were first discussed in Ref. 30. Within the coherent phase approximation (CPA), it was shown that the relaxation time depends linearly on the mean free path, i.e., $\tau \sim \ell / v_F$. For the mean free path, we have $\ell \sim 1 / \sqrt{n_i}$, where n_i stands for the impurity density due to vacancies, cracks, etc. In order to obtain a universal minimal conductivity, the density of states close to the Dirac point must be given by $\rho \sim 1 / (\ell \hbar v_F)$.

This behavior is also obtained from a phenomenological approximation. For this, it is important to note that vacancies give rise to localized states which decay algebraically.¹⁹ These states hybridize due to the overlap with localized states of other vacancies. The energy scale is given by the mean distance between vacancies and approximated by the gain of energy due to the boundary conditions.

This energy scale is approximated as follows. The linearized tight-binding Hamiltonian for a graphene sheet with circular symmetry is given by

$$H_s = \begin{pmatrix} 0 & e^{is\phi} \left(-is\partial_r + \frac{1}{r} \partial_\phi \right) \\ e^{-is\phi} \left(-is\partial_r - \frac{1}{r} \partial_\phi \right) & 0 \end{pmatrix}, \quad (11)$$

where $s = \pm$ denotes the two valleys. At nonzero energy, the general solution is given by the Bessel and Hankel functions. Considering only one valley $s = 1$ and the conduction band, the general wave function in graphene at low energies is thus given by

$$\psi_k(R, \phi) = A \begin{pmatrix} J_0(kR) \\ -iJ_1(kR)e^{i\phi} \end{pmatrix} + B \begin{pmatrix} Y_0(kR) \\ -iY_1(kR)e^{i\phi} \end{pmatrix}. \quad (12)$$

A simple model of surface states at vacancies of radius R_0 which are localized on the radius R_1 now assumes that the first component becomes zero at the inner boundary R_0 and the second component at the outer boundary R_1 , thus assuming zigzag edges on different sublattices. This leads to the following quantization condition for k :

$$J_0(kR_0)Y_1(kR_1) - Y_0(kR_0)J_1(kR_1) = 0. \quad (13)$$

For $kR_1 \ll 1$, the lowest momentum is then given by

$$k \sim \frac{1}{R_1} \frac{1}{\sqrt{|\ln(kR_0)|}}, \quad (14)$$

which defines the width of the localized band

$$E_{\text{loc}} = \frac{\hbar v_F}{R_1 \sqrt{|\ln(R_0/R_1)|}}. \quad (15)$$

The density of states at zero energy is thus approximated by

$$\rho(0) = \frac{\sqrt{|\ln(R_0/R_1)|}}{\hbar v_F R_1}. \quad (16)$$

Since R_1 is related to the average distance between the vacancies, we have $\rho(0) \sim (n_i |\ln n_i|)^{1/2}$. Notice that the CPA calculation of Ref. 30 does not capture the logarithmic correction. We will therefore approximate the density of states as

$$\rho(E) = \alpha \frac{\sqrt{n_i}}{\hbar v_F} g_c(E_{\text{loc}} - |E|) + \frac{2|E|}{\pi(\hbar v_F)^2}, \quad (17)$$

where α is a dimensionless constant of order one and $g_c(E)$ is a cutoff function, e.g., $g_c(E) = \theta(E)$. We note again that we assume a coherent impurity scattering at work, i.e., $\rho(E \rightarrow 0) \sim \sqrt{n_i}$. For clean samples, we would expect the standard scaling behavior, i.e., $\rho(E \rightarrow 0) \sim n_i$.

The density of states of Eq. (17) characterizes two regimes. For high carrier density $E_F > E_{\text{loc}}$, the conductivity of Eq. (9) reads

$$\sigma = \frac{2e^2}{h} v_F k_F \tau_{k_F}. \quad (18)$$

Close to the Dirac point $E_F < E_{\text{loc}}$, we obtain the minimal conductivity

$$\sigma_{\text{min}} = \frac{2\pi e^2}{h} v_F (\alpha \sqrt{n_i}) \tau_{k_F}. \quad (19)$$

Notice that we obtain the same formula as for high electronic densities by introducing a minimal Fermi wave vector $k_{\text{min}} \sim \sqrt{n_i}$. The minimal Fermi wave vector with $k_F \ell \gg 1$ can be related to self-doping effects induced by the very same mechanism which invokes midgap states³⁰ and we will show in the following that a crossover from a linear to constant behavior of the conductivity versus gate voltage takes place.

If one believes that close to the neutrality point the system also behaves in a diffusive way, i.e., that the experimentally observed negatively and positively charged puddles form a

macroscopic network,³¹ then even for low impurity densities $n_i \sim 10^{10} \text{ cm}^{-2}$ with $k_F \ell \approx 1$, one can use our estimates (up to a constant of order 1). Still, we cannot rule out the existence of another regime where the Boltzmann approach is invalid and, e.g., percolation models are at work.³²

Having established the typical behavior of the density of states at the Dirac point due to midgap states, we will discuss several scattering mechanisms.

IV. RELAXATION TIME AND dc CONDUCTIVITY

The collision rate $1/\tau_k$ due to impurity scattering is usually given by³³

$$\frac{1}{\tau_k} = N_i \sum_{k'} \Gamma(\mathbf{k}, \mathbf{k}') (1 - \cos \theta_{\mathbf{k}, \mathbf{k}'}), \quad (20)$$

where N_i is the number of impurities and the transition rate from the quantum state \mathbf{k} to \mathbf{k}' is approximated by Fermi's golden rule

$$\Gamma(\mathbf{k}, \mathbf{k}') = \frac{2\pi}{\hbar} |\langle \mathbf{k} | V_{\text{scatt}} | \mathbf{k}' \rangle|^2 \delta(E_k - E_{k'}). \quad (21)$$

It is only in the scattering matrix $\Gamma(\mathbf{k}, \mathbf{k}')$ where the chirality of the Dirac fermions enters within the Boltzmann formalism. If the scattering potential does not break the sublattice symmetry, this will only lead to a numerical factor. With the Fourier transform of the scattering potential $V_{\text{scatt}}(q)$, the collision rate can then be written as

$$\frac{\hbar}{\tau_{k_F}} = \frac{n_i^{\text{scatt}}}{8} \rho(E_F) \int d\theta |V_{\text{scatt}}(q)|^2 (1 - \cos^2 \theta), \quad (22)$$

where n_i^{scatt} is the impurity density of the scattering potential and $q = 2k_F \sin(\theta/2)$. Notice that the argument of the integral vanishes for both $\theta=0$ and $\theta=\pi$, a situation that does not occur in normal metals.

The effect of vacancies or local impurities with a high potential difference with respect to the graphene layer cannot be treated with the above formulas since they do not capture the change in phase space due to midgap states. We thus determine the relaxation time via the phase shift induced by the scattering center. Assuming elastic scattering and only considering s -wave scattering, the transition rate is then expressed as³³

$$\frac{\hbar}{\tau_k} = \frac{8n_i}{\pi \rho(E_k)} \sin^2(\delta_k), \quad (23)$$

where δ_k is the phase shift of the s -wave channel.

In the following, we will consider various scattering mechanisms, i.e., we will discuss the effect on the electronic conductivity due to (a) local substitutions (short-range ‘‘contact’’ potential), (b) charged impurities in the SiO₂ substrate [long-range (screened) Coulomb potential], and (c) acoustic phonons, where Eqs. (20) and (21) have to be slightly modified. In Sec. IV D, we introduce the scattering mechanism due to midgap states.

Due to the unusually high energies of optical phonons of the order of 0.1–0.2 eV in graphene-related materials, opti-

cal phonons cannot be treated within the Boltzmann formalism since they induce interband transitions for usual densities $n \lesssim 5 \times 10^{12} \text{ cm}^{-2}$. For a discussion on transversal optical phonons in graphene sheets within the Kubo formalism, see Ref. 34.

A. Contact potential

We will first discuss the scattering behavior from $V_{\text{scatt}}(\mathbf{r}) = v_0 \delta(|\mathbf{r}|)$. This yields a relaxation time

$$\tau_k = \frac{8\hbar}{n_i^{\text{contact}} \pi v_0^2 \rho(E_k)} \rightarrow \frac{4\hbar^2 v_F}{n_i^{\text{contact}} v_0^2 k}, \quad (24)$$

where n_i^{contact} is the impurity concentration and the right hand side resembles the high carrier density limit.

Equation (24) can also be obtained from calculating the phase shifts. From Ref. 21, we obtain $\delta_k = v_0 k / (4\hbar v_F)$ in the limit of small k and by expanding Eq. (23) up to linear order in δ_k , we obtain the above result.

The conductivity does not depend on doping³⁵ and we obtain

$$\sigma^{\text{contact}} = \sigma_{\text{min}}^{\text{contact}} = \frac{8e^2}{h} \frac{(\hbar v_F)^2}{n_i^{\text{contact}} v_0^2}. \quad (25)$$

Equation (25) does not depend on an energy scale nor does it lead to a significant contribution for the total conductivity. This is more generally known as the Klein paradox.²²

B. Long-range Coulomb potential

Let us now discuss the influence of the long-range Coulomb potential. Charged impurities reside in the isolating SiO₂ layer and are screened by the conduction electrons of the graphene sheet. This yields for the potential in momentum space³⁶

$$\varphi(q) = \frac{1}{2\epsilon_0 \epsilon q} \rho^{\text{ind}}(q) + \frac{Ze}{2\epsilon_0 \epsilon q} e^{-q|z_c|}, \quad (26)$$

where $\rho^{\text{ind}}(q)$ is the induced charge density, ϵ the permeability of the substrate, and z_c denotes the shortest distance of the external charged impurity to the two-dimensional graphene sheet.

Since we are employing a semiclassical approach, it is consistent to approximate the induced charge density within the Thomas-Fermi (TF) approach,

$$\begin{aligned} \rho^{\text{ind}}(\mathbf{r}) &= -e \frac{4}{A} \sum_{\mathbf{k}} \{f[\epsilon_{\mathbf{k}} - e\varphi(\mathbf{r})] - f(\epsilon_{\mathbf{k}})\} \\ &\approx -e^2 \varphi(\mathbf{r}) \frac{4}{A} \sum_{\mathbf{k}} \left(-\frac{\partial f_k^0}{\partial \epsilon_{\mathbf{k}}} \right) = -e^2 \varphi(\mathbf{r}) \rho(\epsilon_F). \end{aligned} \quad (27)$$

The last equality follows by assuming a Fermi liquid characterized by a sharp Fermi ‘‘surface.’’ For a discussion on nonlinear screening, see Ref. 37.

The TF approach thus gives the following form for the screened potential inside the graphene sheet:

$$\varphi(q) = \frac{Ze}{2\epsilon_0 \epsilon q + \gamma} e^{-q|z_c|}, \quad (28)$$

with $\gamma = \rho(E_F) e^2 / 2\epsilon_0 \epsilon$ and the density of states given by Eq. (17).

At large doping, we have $\gamma = \tilde{\gamma} k_F$ and from Eq. (22) with $V_{\text{scatt}}(q) = e\varphi(q)$ and $z_c \approx 0$, we obtain

$$\tau_{k_F} = \frac{\hbar^2 v_F k_F}{u_0^2} \quad \text{with } u_0 = \frac{\sqrt{n_i^C} Ze^2}{4\epsilon_0 \epsilon (1 + \tilde{\gamma})}, \quad (29)$$

where n_i^C is the density of charged impurities in the sample. This leads to the following conductivity:

$$\sigma^{\text{Coulomb}} = \frac{2e^2}{h} \frac{(\hbar v_F k_F)^2}{u_0^2}. \quad (30)$$

Equations (29) and (30) are slightly modified for $z_c > 0$.¹⁴

At zero doping, we obtain the minimal conductivity

$$\sigma_{\text{min}}^{\text{Coulomb}} \rightarrow \frac{4e^2}{h} \frac{n_i}{n_i^C} (2\alpha)^2. \quad (31)$$

We thus find a universal behavior at low doping if $n_i \approx n_i^C$. For $\alpha = 1/2$, we obtain the experimentally observed value of $\sigma = 4e^2/h$.

Now, we want to determine the numerical values of the relaxation times due to charged impurities and later compare them to the ones due to acoustic phonon scattering. Let us assume that the electronic density in the graphene sample, induced by the gate voltage, has the typical value (gate voltage of 100 V)¹

$$n = 7.2 \times 10^{12} \text{ cm}^{-2}. \quad (32)$$

The Fermi momentum is given by $n = k_F^2 / \pi$, where contributions from both spins and both Dirac points were included; this leads to a value for k_F given by

$$k_F = 4.8 \times 10^8 \text{ m}^{-1}. \quad (33)$$

With $e^2/4\pi\epsilon_0 = 14.4 \text{ eV \AA}$ and $\hbar v_F = 3at/2 = 5.75 \text{ eV \AA}$, where $a = 1.42 \text{ \AA}$ and $t = 2.7 \text{ eV}$, we find for large densities $\gamma = 10k_F/\epsilon$. For $Z = 1$ and $z_c \approx 0$, we set $\epsilon = 2.4$, which is the average of the dielectric constant of SiO₂ and vacuum since the graphene layer is sandwiched by these two layers. For large carrier densities, we thus have $\gamma = \tilde{\gamma} k_F$ with $\tilde{\gamma} \approx 4.2$.

Using Eq. (29) and the above value for k_F , we obtain

$$\tau_{k_F} \approx 6 \times 10^{-17} (\bar{n}_i^C)^{-1} \text{ s}, \quad (34)$$

where \bar{n}_i^C is the concentration of impurities per unit cell. Since it has been experimentally determined that the mean free path ℓ of electrons in graphene can be as large as $0.3 \mu\text{m}$, the experimental relaxation time is seen to be of the order of

$$\tau \approx \frac{\ell}{v_F} \approx 3 \times 10^{-13} \text{ s}. \quad (35)$$

This last result implies that the concentration of impurities per unit cell has a value of the order of

$$\bar{n}_i^C \approx 2 \times 10^{-4}, \quad (36)$$

if one only assumes the Coulomb scattering mechanism. This corresponded to a density of $n_i^C = 4 \times 10^{11} \text{ cm}^{-2}$ and a mobility of $11\,100 \text{ cm}^2/\text{V s}$. However, note that graphene normally exhibits lower mobilities for which a higher impurity density is necessary.¹ Also, finite z_c and a higher dielectric constant, e.g., $\epsilon = 3.9$ which holds for SiO_2 , lead to a larger relaxation time and thus imply higher impurity concentrations to match the experimental results. In summary, we strongly believe that the Coulomb scattering mechanism is only capable to explain a marginal fraction of the observed data.

C. Phonons

The relaxation time τ_k for phonon scattering is defined as

$$\frac{1}{\tau_k} = \sum_{\mathbf{k}'} \Gamma(\mathbf{k}, \mathbf{k}') (1 - \cos \theta), \quad (37)$$

where the transition rate $\Gamma(\mathbf{k}, \mathbf{k}')$ is given by

$$\Gamma(\mathbf{k}, \mathbf{k}') = \frac{2\pi}{\hbar} |H_{\mathbf{k}', \mathbf{k}}|^2 \delta(v_F \hbar k' - v_F \hbar k - \hbar \omega), \quad (38)$$

where $v_F \hbar k$ is the dispersion of Dirac fermions in graphene, $\hbar \omega$ the phonon energy, and $H_{\mathbf{k}', \mathbf{k}}$ is defined as

$$H_{\mathbf{k}', \mathbf{k}} = \int d^2 r \psi_{\mathbf{k}'}^*(\mathbf{r}) U_S(\mathbf{r}) \psi_{\mathbf{k}}(\mathbf{r}), \quad (39)$$

with $U_S(\mathbf{r})$ the scattering potential and $\psi_{\mathbf{k}}(\mathbf{r})$ is the electronic wave function of a clean graphene sheet.

If the potential is due to the propagation of phonons, it has the form³⁸

$$U_S = K_q A_q e^{i(\mathbf{q} \cdot \mathbf{r} - \omega t)}, \quad (40)$$

where³⁸

$$|K_q|^2 = D_A^2 q^2, \quad (41)$$

$$|A_q|^2 = \frac{\hbar}{2\rho A \omega_q} N(\omega_q), \quad (42)$$

$$N(\omega_q) = \frac{1}{e^{\hbar \omega_q / (k_B T)} - 1} \approx \frac{k_B T}{\hbar \omega_q}, \quad (43)$$

where ρ is the density of graphene and D_A is the electron acoustic deformation potential, estimated to be of the order of $3t$, where t is the first neighbor hopping matrix in graphene of the order of 3 eV .³⁹ A similar estimate for the deformation potential is obtained by relating the bond length with the hopping amplitude.⁴⁰

The matrix element $H_{\mathbf{k}', \mathbf{k}}$ is easily obtained as

$$H_{\mathbf{k}', \mathbf{k}} = \cos(\theta/2) K_q A_q \delta_{\mathbf{k}+\mathbf{q}, \mathbf{k}'} e^{-i\omega t}. \quad (44)$$

Using Eq. (44) in Eq. (38), the transition rate $\Gamma(\mathbf{k}, \mathbf{k}')$ reads

$$\Gamma(\mathbf{k}, \mathbf{k}') = \frac{\pi}{\hbar} |K_q|^2 |A_q|^2 (1 + \cos \theta) \delta_{\mathbf{k}+\mathbf{q}, \mathbf{k}'} \times \delta(v_F \hbar k' - v_F \hbar k - \hbar \omega_q). \quad (45)$$

The form of $\Gamma(\mathbf{k}, \mathbf{k}')$ represents the absorption of a phonon of momentum \mathbf{q} and energy $\hbar \omega_q$. Since we want to describe the absorption of acoustic phonons, we write the dispersion ω_q as

$$\omega_q = v_S q, \quad (46)$$

where v_S is the sound velocity. The conservation of momentum, $\mathbf{k} + \mathbf{q} = \mathbf{k}'$, leads to

$$q = \sqrt{k'^2 + k^2 - 2k'k \cos \theta}, \quad (47)$$

which allows us to write the product of the Kronecker symbol and the Dirac delta function as a single delta function, which reads

$$\delta(v_F \hbar k' - v_F \hbar k - \hbar v_S \sqrt{k'^2 + k^2 - 2k'k \cos \theta}). \quad (48)$$

Since $v_F \gg v_S$, the argument of the delta function [Eq. (48)] can be approximated by $v_F \hbar k' - v_F \hbar k$, i.e., the absorption of acoustic phonons can be seen as a quasielastic scattering process.

The final result for the scattering time is

$$\tau_k \approx \frac{8\hbar^2 \rho v_S^2 v_F}{D_A^2 k_B T} \frac{1}{k}, \quad (49)$$

which is formally similar to the relaxation time produced by a contact potential [Eq. (24)] except for the temperature dependence which is absent in the latter case.

Let us now concentrate on the numerical values of the relaxation time due to phonons. The phonon spectrum of graphene has two acoustic branches named *LA*, with a velocity of $7.33 \times 10^3 \text{ m/s}$, and *TA*, with a velocity of $2.82 \times 10^3 \text{ m/s}$.⁴¹ At the temperature of 1 K , the relaxation times of these two modes are

$$\tau_{LA} \approx 2.7 \times 10^{-10} \text{ s}, \quad (50)$$

$$\tau_{TA} \approx 4.0 \times 10^{-11} \text{ s}, \quad (51)$$

which are clearly much larger than the estimated value of $3 \times 10^{-13} \text{ s}$. Therefore, at this low temperatures, the scattering is mainly dominated by impurities. At temperatures around 100 K , the scattering lifetime diminishes by a factor of 100 , leading to values comparable to that obtained from the scattering from charged impurities. Considering only charged impurities as the scattering mechanism, the effect of phonons on the transport properties of graphene must be taken into account if the calculations of the transport coefficients are extended to temperatures of the order of or above 100 K .

Let us finally discuss the effect of temperature on the need of taking into account thermal excitations of the valence band into the conduction band. For the value of the Fermi momentum given above, the Fermi energy has a value of $\hbar v_F k_F = 0.3 \text{ eV}$. This energy value corresponds to a temperature of the order of 3600 K . Therefore, as long as the tem-

perature is much smaller than this value, the valence band can be considered as inert and therefore we can perform the calculations by neglecting the effect of the valence band altogether.

D. Vacancies

Vacancies, cracks, or boundaries in the graphene sheet give rise to bound states at the Dirac point, so-called midgap states. This is also true for corrugated graphene. There is thus inherent disorder in the system that has to be treated adequately. The influence of midgap states is not captured in Eqs. (20) and (21), where the reference point is given by the unperturbed system described by plane (spinor) waves, i.e., $\psi_{\mathbf{k}}(\mathbf{r}) = \langle \mathbf{x} | \mathbf{k} \rangle$ is the electronic wave function of a *clean* graphene sheet. This is also the reason why the Klein paradox is not at work, which would render scattering from local impurities (i.e., vacancies) irrelevant.

In order to incorporate the effect of midgap states in the calculation of the relaxation time, we depart from Eq. (23). Scattering from vacancies leads to the following phase shift:²¹

$$\delta_k = -\frac{\pi}{2} \frac{1}{\ln(kR_0)}. \quad (52)$$

This means that for $kR_0 \ll 1$,

$$\tau_k = \frac{\hbar \rho(E_k)}{2\pi n_i} (\ln kR_0)^2. \quad (53)$$

For large carrier densities, $\rho(E_k) \sim k$, and apart from the logarithmic correction, this is the scattering behavior coming from long-range Coulomb potentials.^{9,10,42} Explicitly, one obtains

$$\tau_k = \frac{k}{\pi^2 v_F n_i} (\ln kR_0)^2. \quad (54)$$

The logarithmic correction leads to a sublinear density dependence of the conductivity

$$\sigma^{\text{vacancies}} = \frac{e^2}{h} \frac{2}{\pi} k_F^2 (\ln k_F R_0)^2. \quad (55)$$

We note that the same behavior is obtained if one includes wiggles and thus a random magnetic field in the graphene sheet.²³ The relation between midgap states and corrugated graphene was investigated in Ref. 20.

The vacancies induce midgap states.⁴³ In the presence of terms which break the electron-hole symmetry, these states become completely filled or are empty, leading to self-doping effects.³⁰ Hence, the carrier density, $n \propto k_F^2$, is bounded by the concentration of vacancies, n_i . When the gate voltage is tuned near the neutrality point, the conductivity then becomes almost independent of the gate voltage, $\sigma \sim \ln(k_F a) \sim \ln(\bar{n}_i)$, with a prefactor of order e^2/h . Note that this argument relies on the existence of a finite carrier density $n \propto n_i$, and since the mean free path $\ell \sim k_F^{-1} \ln(k_F a)$ can be longer than k_F^{-1} due to $|\ln(k_F a)| \approx 10$, the Boltzmann equation remains valid.

The previous argument breaks down when the gate voltage is such that the localized states induced by the vacancies become partially filled. The formation of charge puddles will limit the validity of our analysis near the neutrality point.

To summarize our analysis in the limit of low carrier densities, we obtain with $k_{\min} \sim n_i^{1/2}$ the following result for the minimal conductivity ($n_i = \bar{n}_i/A_c$ and $R_0^2 \sim A_c$):

$$\sigma_{\min}^{\text{vacancies}} = \frac{e^2}{h} (\alpha |\ln \bar{n}_i|)^2. \quad (56)$$

Notice that there is no ‘‘linear’’ dependence of the impurity density \bar{n}_i . Having a typical impurity density per unit cell of $\bar{n}_i = 10^{-4}$, which matches well the experimentally observed mobility, the logarithmic correction can be approximated as $|\ln \bar{n}_i| \approx 8$. For $\alpha = 1/4$, we obtain the experimentally observed minimal conductivity $\sigma_{\min} = 4e^2/h$.

For cleaner samples, the logarithmic correction has to be taken into account. This is in accordance to experimental findings which show higher conductivity for cleaner samples.^{15,44}

V. OTHER TRANSPORT QUANTITIES

In Ref. 42, predictions were made on how the ac conductivity, the thermal conductivity and the thermopower depend on the carrier density if one assumes the scattering behavior $\tau_k \sim k$. The scattering mechanism from vacancies, cracks, or boundaries yields a different scattering behavior, i.e., $\tau_k \sim k(\ln kR_0)^2$. In the following, we give the density dependence in terms of the Fermi energy $E_F = \hbar v_F k_F$ for the above quantities assuming this scattering mechanism at work ($n = E_F^2/\pi$). Measuring these quantities may then disclose which scattering mechanism dominates.

A. Optical conductivity

Here, we want to obtain the electronic density dependence of the optical conductivity of a doped graphene plane. Since the Boltzmann approach does not include interband transitions, the expressions obtained below are only valid as long as $\hbar\omega \leq E_F$ with $E_F = \hbar v_F k_F$ the Fermi energy, where the above mentioned transitions are blocked by the Pauli principle.

Our aim is to obtain the response of the electronic system to an external electric field of the form

$$\mathbf{E} = \mathbf{E}_0 e^{i(\mathbf{q}\cdot\mathbf{r} - \omega t)}. \quad (57)$$

The Boltzmann equation has, for this problem, the form

$$-\frac{\partial f^0(\epsilon_{\mathbf{k}})}{\partial \epsilon_{\mathbf{k}}} e \mathbf{v}_{\mathbf{k}} \cdot \mathbf{E} = \frac{g_{\mathbf{k}}}{\tau_{\mathbf{k}}} + \mathbf{v}_{\mathbf{k}} \cdot \nabla_{\mathbf{r}} g_{\mathbf{k}} + \frac{\partial g_{\mathbf{k}}}{\partial t}. \quad (58)$$

The solution of the linearized Boltzmann equation [Eq. (58)] is well known,²⁸ which reads

$$g_{\mathbf{k}} = -\frac{\partial f^0(\epsilon_{\mathbf{k}})}{\partial \epsilon_{\mathbf{k}}} \Phi_{\mathbf{q}}(\omega, \mathbf{k}) e^{i(\mathbf{q}\cdot\mathbf{r} - \omega t)}, \quad (59)$$

with

$$\Phi_q(\omega, \mathbf{k}) = \frac{e\tau_k \mathbf{v}_k \cdot \mathbf{E}_0}{1 - i\omega\tau_k + i\tau_k \mathbf{q} \cdot \mathbf{v}_k}. \quad (60)$$

The Fourier component $\mathbf{J}(\omega, \mathbf{q})$ of the current is given by

$$\mathbf{J}(\omega, \mathbf{q}) = \frac{1}{\pi^2} \int d^2k e \mathbf{v}_k \Phi_q(\omega, \mathbf{k}) \left[-\frac{\partial f^0(\epsilon_k)}{\partial \epsilon_k} \right], \quad (61)$$

leading in the long-wavelength limit to an optical conductivity of the form

$$\sigma(\omega) = 2 \frac{e^2 E_F^2}{h \tilde{u}_0^2} (\ln E_F / \tilde{v}_0)^2 \frac{1 + i \frac{\omega \hbar E_F}{\tilde{u}_0^2} (\ln E_F / \tilde{v}_0)^2}{1 + \left[\frac{\omega \hbar E_F}{\tilde{u}_0^2} (\ln E_F / \tilde{v}_0)^2 \right]^2}. \quad (62)$$

In the above equation, we defined the two energy scales $\tilde{u}_0^2 = \pi^2 n_i \hbar^2 v_F^2$ and $\tilde{v}_0 = \hbar v_F / R_0$. What should be stressed about Eq. (62) is its density dependence $n = E_F^2 / \pi$.

B. Thermal conductivity and thermopower

In the presence of a temperature gradient in the sample, the linearized Boltzmann equation has the form

$$-\frac{\partial f^0(\epsilon_k)}{\partial \epsilon_k} \mathbf{v}_k \cdot \left[\left(-\frac{\epsilon_k - E_F}{T} \right) \nabla_r T + e \mathbf{E}_{obs} \right] = \frac{g_k}{\tau_k}, \quad (63)$$

where the measured electric field is given by $\mathbf{E}_{obs} = \mathbf{E} - \nabla_r E_F / e$. In this situation, we have, in addition to the electric current, a heat current (flux of heat per unit of area) given by

$$\mathbf{U} = \frac{4}{A} \sum_k \mathbf{v}_k (\epsilon_k - E_F) g_k. \quad (64)$$

Both the electric and the heat currents can be written as²⁸

$$\mathbf{J} = e^2 \mathbf{K}_0 \cdot \mathbf{E}_{obs} + \frac{e}{T} \mathbf{K}_1 \cdot (-\nabla_r T), \quad (65)$$

$$\mathbf{U} = e \mathbf{K}_1 \cdot \mathbf{E}_{obs} + \frac{1}{T} \mathbf{K}_2 \cdot (-\nabla_r T),$$

where \mathbf{K}_i , $i=0, 1, 2$ are second order tensors. In this problem, the tensors are diagonal, i.e., $\mathbf{K}_i = \mathbf{1} k_i$, and by a well established procedure,²⁸ one obtains

$$k_0 = \frac{2 E_F^2}{h \tilde{u}_0^2} (\ln E_F / \tilde{v}_0)^2, \quad (66)$$

$$k_1 = \frac{4 \pi^2}{3 h} (k_B T)^2 \frac{E_F}{\tilde{u}_0^2} (\ln E_F / \tilde{v}_0)^2 [1 + (\ln E_F / \tilde{v}_0)^{-1}], \quad (67)$$

$$k_2 = \frac{2 \pi^2}{3 h} (k_B T)^2 \frac{E_F^2}{\tilde{u}_0^2} (\ln E_F / \tilde{v}_0)^2. \quad (68)$$

In the above equations, we defined the two energy scales $\tilde{u}_0^2 = \pi^2 n_i \hbar^2 v_F^2$ and $\tilde{v}_0 = \hbar v_F / R_0$.

From the results [Eqs. (66)–(68)], it is easy to derive both the thermal conductivity κ and the thermopower Q . These are given by

$$\kappa = \frac{1}{T} \left[\frac{2 \pi^2}{3 h} (k_B T)^2 \frac{E_F^2}{u_0^2} (\ln E_F / \tilde{v}_0)^2 - \frac{8 \pi^4}{9 h} (k_B T)^4 \frac{1}{u_0^2} (1 + \ln E_F / \tilde{v}_0) \right] \quad (69)$$

and

$$Q = \frac{1}{e T} \frac{2 \pi^2}{3 E_F} (k_B T)^2 [1 + (\ln E_F / \tilde{v}_0)^{-1}]. \quad (70)$$

Again, what should be emphasized in these results is the dependence of both κ and Q on the particle density, which is different from that of the usual two-dimensional electron gas and from the graphene sheet with only charged impurities in the substrate. Since it is experimentally feasible to control the carrier density in the graphene plane,¹ it is possible to check experimentally the dependence of the transport coefficients on the particle density. Finding the logarithmic corrections compared to the Coulomb scattering mechanism will be a strong indication for scattering due to midgap states.

Normally, the second term of Eq. (69) can be safely neglected and one obtains the well-known Wiedemann-Franz law

$$\kappa = \frac{\pi^2 k_B^2}{3 e^2} T \sigma. \quad (71)$$

However, due to the logarithmic correction in the scattering time, there is an additional term in k_1 , usually not present and thus a modified second term in Eq. (69). So, even though our analysis is only valid for $E_F / \tilde{v}_0 \ll 1$, we expect the Wiedemann-Franz law to be modified for large carrier densities.

VI. NUMERICAL RESULTS

A. Phonon contribution

We now use the obtained values for the relaxation times of phonon scattering to compute the conductivity at finite temperatures including scattering from charged impurities. Since there are two different mechanisms, the total relaxation time is

$$\frac{1}{\tau_{k_F}} = \frac{u_0^2}{v_F \hbar^2 k_F} + \frac{D_A^2 k_B T}{8 \hbar^2 \rho v_s^2 v_F} k_F = \frac{\alpha_1}{k_F} + \alpha_2 k_F, \quad (72)$$

where u_0 was defined in Eq. (29) with $Z=1$, $\epsilon=2.4$, and $\tilde{\gamma}=4.2$.

The conductivity, including the contribution from two Dirac cones, reads

$$\sigma = 2 \frac{e^2 E_F k_F}{h 4 k_B T} \int_0^\infty \frac{x^2 dx}{\alpha_1 + \alpha_2 k_F^2 x^2} \cosh^{-2} \left(\frac{E_F x - \mu}{2 k_B T} \right), \quad (73)$$

where $E_F = v_F \hbar k_F$. The integral has a maximum around $x=1$ and can be done numerically. The chemical potential de-

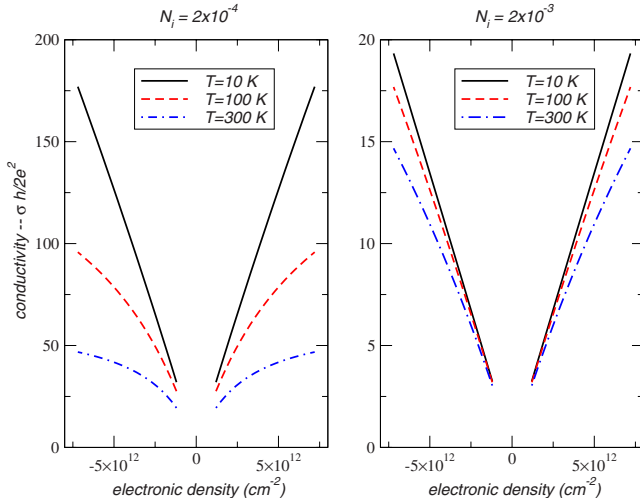


FIG. 1. (Color online) Conductivity as a function of the electronic density, for different values of temperature and for two impurity concentrations: (left) $\bar{n}_i = 2 \times 10^{-4}$ and (right) $\bar{n}_i = 2 \times 10^{-3}$.

depends on the temperature and in the temperature range of $T \in 1-300$ K is well described by the asymptotic expression

$$\mu \simeq \epsilon_F - \frac{(\pi k_B T)^2}{6E_F}. \quad (74)$$

In Fig. 1, the conductivity as a function of the electronic density is shown for different values of temperature and for two impurity concentrations $\bar{n}_i = 2 \times 10^{-4}$ (left hand side) and $\bar{n}_i = 2 \times 10^{-3}$ (right hand side). In Fig. 2, the conductivity as a function of temperature is shown, for two impurity concentrations $\bar{n}_i = 2 \times 10^{-3}$ (upper panels) and $\bar{n}_i = 2 \times 10^{-4}$ (lower panels), and for two different electronic densities $n = 7.2 \times 10^{12} \text{ cm}^{-2}$ (left hand side) and $n = 1.2 \times 10^{12} \text{ cm}^{-2}$ (right hand side).

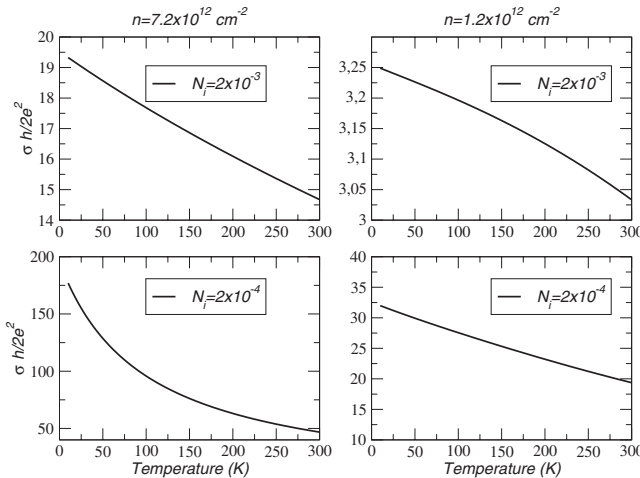


FIG. 2. Conductivity as a function of temperature, for two impurity concentrations (up) $\bar{n}_i = 2 \times 10^{-3}$ and (down) $\bar{n}_i = 2 \times 10^{-4}$ and for two different electronic densities (left) $n = 7.2 \times 10^{12} \text{ cm}^{-2}$ and (right) $n = 1.2 \times 10^{12} \text{ cm}^{-2}$.

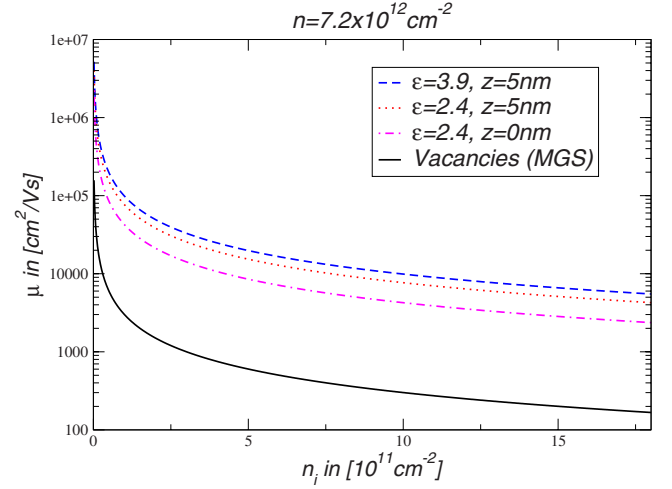


FIG. 3. (Color online) The mobility $\mu = \sigma/ne$ in units of $\text{cm}^2/\text{V s}$ due to Coulomb scatterers with $\epsilon = 3.9, 2.4, z = 5$ nm, and $\epsilon = 2.4, z = 0$ (upper three lines), and vacancies as a function of the impurity density for a carrier density $n = 7.2 \times 10^{12} \text{ cm}^{-2}$ (full line).

For low impurity density, i.e., for realistic parameters, there is a striking temperature effect on the conductivity which is not seen in the experiment. We, therefore, conclude once again that charged impurity cannot resemble the main scattering mechanism.

B. Influence of midgap states

There are different estimates for the density of (charged) impurities. Preparing the Si-SiO₂ wafer by oxidizing the *n*-doped silicon wafer produces no relevant impurity density, which would affect the transport properties of graphene. This is because charges due to dangling bonds are mainly localized between the Si-SiO₂ interface and thus exponentially suppressed due to the 300 nm thick SiO₂ layer.^{17,45} Placing the graphene sheet by micromechanical cleavage on top of the wafer might produce ionization of the OH groups, which neutralize the SiO₂ surface. We estimate a (relevant) charged impurity concentration of $n_i^C \leq 10^{11} \text{ cm}^{-2}$.⁴⁶

The estimates for the impurity density of vacancies are even lower, having in mind the high energy cost of three missing bonds. Nevertheless, the main observation of this work is that midgap states give rise to a similar scattering behavior as long-range Coulomb scatterers. Midgap states can also occur from cracks or boundaries. Another realization comes from impurities with large potential difference with respect to the graphene sheet or corrugated graphene. We summarize all these effects in the impurity density $n_i \leq 10^{11} \text{ cm}^{-2}$ and set $R_0 \sim 1.4 \text{ \AA}$.

Figure 3 shows the mobility $\mu = \sigma/ne$ at a carrier density of $7.2 \times 10^{12} \text{ cm}^{-2}$, which corresponds to a gate voltage of $V_g = 100$ V. The upper three curves show the mobility due to Coulomb scattering, where the dielectric constant ϵ and the average distance to the graphene sheet are varied. The lower curve (full line) shows the mobility due to vacancies. Vacancies yield the lowest mobility for comparable impurity densities and thus represent the dominant scattering process.

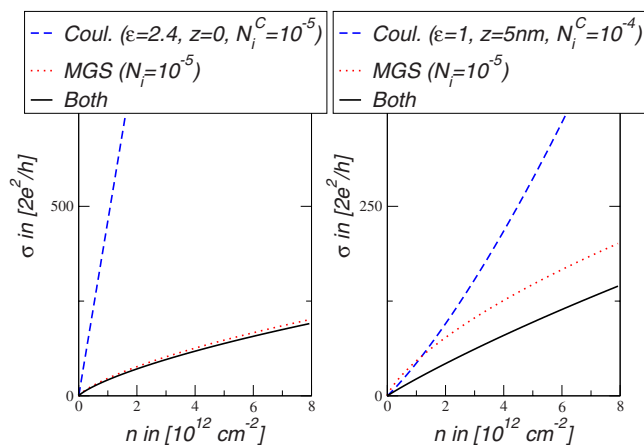


FIG. 4. (Color online) The left hand side shows the conductivity due to Coulomb scatterers with $\epsilon=2.4$, $z=0$, and $n_i^C=2 \times 10^{10} \text{ cm}^{-2}$ (dashed line), vacancies with $n_i=2 \times 10^{10} \text{ cm}^{-2}$ (mid-gap states) (dotted line), and both contributions (full line). The right hand side shows the same plots with different Coulomb scatterers with $\epsilon=1$, $z=5 \text{ nm}$, and $n_i^C=2 \times 10^{11} \text{ cm}^{-2}$.

In Fig. 4, the conductivity is shown as a function of the carrier density n . The left hand side shows the conductivity due to Coulomb scattering with $\epsilon=2.4$, $z_c=0$, and $n_i^C=2 \times 10^{10} \text{ cm}^{-2}$ (dashed line), vacancies with $n_i=2 \times 10^{10} \text{ cm}^{-2}$ (dotted line), and due to both contributions (full line). The right hand side shows the same plots with different Coulomb scatterers, i.e., with $\epsilon=1$, $z_c=5 \text{ nm}$, and $n_i^C=2 \times 10^{11} \text{ cm}^{-2}$.

The conductivity of the cleaner sample (left hand side) is not affected by the Coulomb scattering mechanism and shows a sublinear behavior in the electronic density. For the dirty sample (right hand side) with $z_c=5 \text{ nm}$, i.e., the charged impurities are well inside the substrate, the Coulomb scattering mechanism leads to a superlinear behavior, which in total yields the linear behavior of the combined conductivity with respect to the carrier density n . The above parameters yield mobilities of $\mu \approx 12000 \text{ cm}^2/\text{V s}$ (left) and $\mu \approx 8800 \text{ cm}^2/\text{V s}$ (right).

VII. CONCLUSIONS

In summary, we presented a phenomenological theory for transport in graphene based on the semiclassical Boltzmann theory, first proposed by Nomura and MacDonald.⁹ We pointed out that local point defects in the form of vacancies, cracks, etc., yield a similar k dependence of the relaxation time as long-range Coulomb potentials. Moreover, they lead to a finite density of states at the Dirac point, which can account for the observed minimal conductivity. The scattering mechanism due to midgap states has been widely ignored so far but actually represents the dominant contribution to the total conductivity.

For dirty samples, this scattering mechanism yields a universal minimal conductivity, whereas for cleaner samples, the minimal conductivity increases logarithmically in the impurity density. It also leads to a sub-linear behavior with respect to the carrier density. In combination with Coulomb scattering, this behavior may become linear.

Regarding the numerical values, the major uncertainty lies in the impurities densities of charged or neutral defects. Cleaning the SiO_2 surface in a hydroxyl bath^{46,47} would reduce charged impurities close to the graphene sheet and thus estimate their effect to the conductivity. Another way of reducing a possible source of impurities is by interchanging the mechanical cleavage by “printing” the graphene sheet on top of the substrate.⁴⁸

ACKNOWLEDGMENTS

The authors want to thank J. M. B. Lopes dos Santos, S.-W. Tsai, and A. H. Castro Neto for useful comments and many discussions. N.M.R.P. acknowledges discussions with M. Vasilevskiy and T.S. with C. Seoáñez. This work has been supported by MEC (Spain) through Grant No. FIS2004-06490-C03-00, by the European Union, through Contract No. 12881 (NEST), and the Juan de la Cierva Program (MEC, Spain). N.M.R.P. thanks FCT under the Grant No. PTDC/FIS/64404/2006.

¹K. S. Novoselov, A. K. Geim, S. V. Morozov, D. Jiang, Y. Zhang, S. V. Dubonos, I. V. Grigorieva, and A. A. Firsov, *Science* **306**, 666 (2004).

²K. S. Novoselov, A. K. Geim, S. V. Morozov, D. Jiang, M. I. Katsnelson, I. V. Grigorieva, S. V. Dubonos, and A. A. Firsov, *Nature (London)* **438**, 197 (2005).

³Y. Zhang, Y.-W. Tan, H. L. Stormer, and P. Kim, *Nature (London)* **438**, 201 (2005).

⁴F. Schedin, A. K. Geim, S. V. Morozov, D. Jiang, E. H. Hill, P. Blake, and K. Novoselov, *Nat. Mater.* **6**, 652 (2007).

⁵A. K. Geim and K. S. Novoselov, *Nat. Mater.* **6**, 183 (2007).

⁶M. I. Katsnelson, *Mater. Today* **10**, 20 (2007).

⁷A. H. Castro Neto, F. Guinea, and N. M. R. Peres, *Phys. World* **19**, 33 (2006).

⁸A. K. Geim and A. H. MacDonald, *Phys. Today* **60**(8), 35 (2007).

⁹K. Nomura and A. H. MacDonald, *Phys. Rev. Lett.* **96**, 256602 (2006).

¹⁰E. H. Hwang, S. Adam, and S. Das Sarma, *Phys. Rev. Lett.* **98**, 186806 (2007).

¹¹S. Y. Liu, X. L. Lei, and N. J. M. Horing, arXiv:0707.0559 (unpublished).

¹²J. H. Chen, C. Jang, M. S. Fuhrer, E. D. Williams, and M. Ishigami, arXiv:0708.2408 (unpublished).

¹³E. H. Hwang, S. Adam, S. Das Sarma, and A. K. Geim, arXiv:cond-mat/0610834 (unpublished).

¹⁴S. Adam, E. H. Hwang, V. M. Galitski, and S. Das Sarma, arXiv:0705.1540 (unpublished).

¹⁵Y.-W. Tan, Y. Zhang, K. Bolotin, Y. Zhao, S. Adam, E. H. Hwang, S. Das Sarma, H. L. Stormer, and P. Kim, arXiv:0707.1807 (unpublished).

- ¹⁶K. Nomura and A. H. MacDonald, Phys. Rev. Lett. **98**, 076602 (2007).
- ¹⁷Y. Wu and M. Shannon, J. Micromech. Microeng. **14**, 989 (2004).
- ¹⁸M. Fujita, K. Wakabayashi, K. Nakada, and K. Kusakabe, J. Phys. Soc. Jpn. **65**, 1920 (1996).
- ¹⁹M. A. H. Vozmediano, M. P. López-Sancho, T. Stauber, and F. Guinea, Phys. Rev. B **72**, 155121 (2005).
- ²⁰F. Guinea, M. I. Katsnelson, and M. A. H. Vozmediano, arXiv:0707.0682 (unpublished).
- ²¹M. Hentschel and F. Guinea, arXiv:0705.0522 (unpublished).
- ²²M. I. Katsnelson and K. S. Novoselov, Solid State Commun. **143**, 3 (2007).
- ²³M. I. Katsnelson and A. K. Geim, Philos. Trans. R. Soc. London, Ser. A (to be published).
- ²⁴B. Wunsch, T. Stauber, F. Sols, and F. Guinea, New J. Phys. **8**, 318 (2006).
- ²⁵E. H. Hwang and S. Das Sarma, Phys. Rev. B **75**, 205418 (2007).
- ²⁶H. Bruus and K. Flensberg, *Many-Body Quantum Theory in Condensed Matter Physics* (Oxford University, New York, 2004).
- ²⁷M. Auslender and M. I. Katsnelson, arXiv:0707.2804 (unpublished).
- ²⁸J. M. Ziman, *Principles of the Theory of Solids*, 2nd ed. (Cambridge University, Cambridge, 1972).
- ²⁹A. W. W. Ludwig, M. P. A. Fisher, R. Shankar, and G. Grinstein, Phys. Rev. B **50**, 7526 (1994).
- ³⁰N. M. R. Peres, F. Guinea, and A. H. Castro Neto, Phys. Rev. B **73**, 125411 (2006).
- ³¹J. Martin, N. Akerman, G. Ulbricht, T. Lohmann, J. H. Smet, K. von Klitzing, and A. Yacoby, arXiv:0705.2180 (unpublished).
- ³²V. V. Cheianov, V. I. Fal'ko, B. L. Altshuler, and I. L. Aleiner, arXiv:0706.2968 (unpublished).
- ³³G. D. Mahan, *Many-Particle Physics*, 3rd ed. (Plenum, New York, 2000).
- ³⁴T. Stauber and N. M. R. Peres, arXiv:0707.4248 (unpublished).
- ³⁵T. Ando, J. Phys. Soc. Jpn. **75**, 074716 (2006).
- ³⁶P. B. Visscher and L. M. Falicov, Phys. Rev. B **3**, 2541 (1971).
- ³⁷M. I. Katsnelson, Phys. Rev. B **74**, 201401(R) (2006).
- ³⁸Mark Lundstron, *Fundamentals of Carrier Transport*, 2nd ed. (Cambridge University, Cambridge, 2000).
- ³⁹G. Pennington and N. Goldsman, Phys. Rev. B **68**, 045426 (2003).
- ⁴⁰A. H. Castro Neto and F. Guinea, Phys. Rev. B **75**, 045404 (2007).
- ⁴¹L. A. Falkovsky, arXiv:cond-mat/0702409 (unpublished).
- ⁴²N. M. R. Peres, J. M. B. Lopes dos Santos, and T. Stauber, Phys. Rev. B **76**, 073412 (2007).
- ⁴³V. M. Pereira, F. Guinea, J. M. B. Lopes dos Santos, N. M. R. Peres, and A. H. Castro Neto, Phys. Rev. Lett. **96**, 036801 (2006).
- ⁴⁴F. Miao, S. Wijeratne, U. Coskun, Y. Zhang, and C. N. Lau, arXiv:cond-mat/0703052 (unpublished).
- ⁴⁵A. I. Ankinwande and J. D. Plummer, J. Electrochem. Soc. **134**, 2565 (1987); **134**, 2573 (1987).
- ⁴⁶O. Sneh and S. M. George, J. Phys. Chem. **99**, 4639 (1995).
- ⁴⁷M. J. Wirth, R. W. P. Fairbank, and H. O. Fatunmbi, Science **275**, 44 (1997).
- ⁴⁸N. Agraït (private communication).